ChemComm

Chemical Communications

www.rsc.org/chemcomm
Volume 48 | Number 35 | 4 May 2012 | Pages 4129–4260

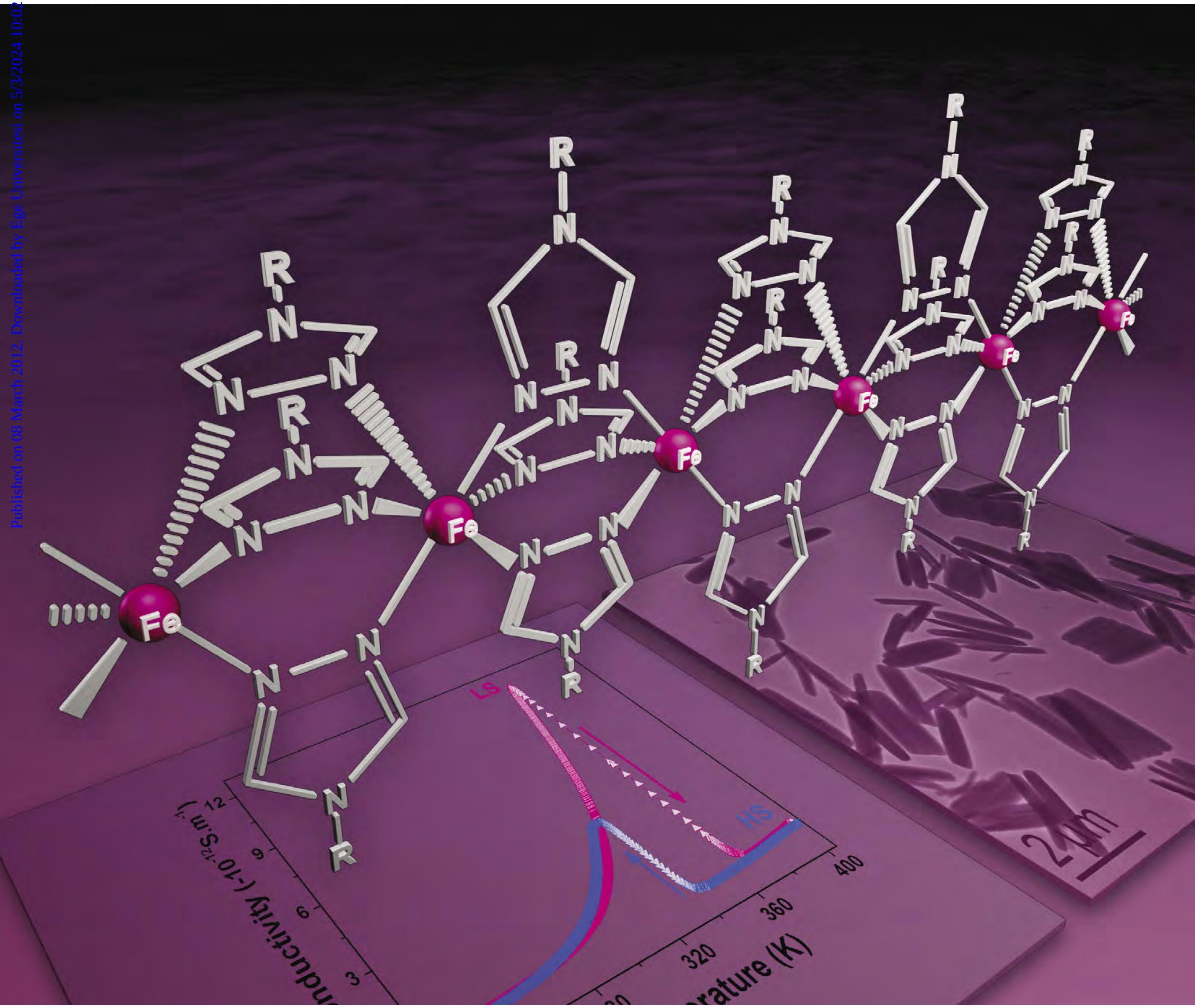

ISSN 1359-7345

RSCPublishing

COMMUNICATION
Bousseksou *et al.*
Spin state dependence of electrical conductivity of spin crossover materials

1359-7345(2012)48:35;1-6

ChemComm

Cite this: *Chem. Commun.*, 2012, **48**, 4163–4165

www.rsc.org/chemcomm

COMMUNICATION

Spin state dependence of electrical conductivity of spin crossover materials†

Aurelian Rotaru,[ab] Il'ya A. Gural'skiy,[ac] Gábor Molnár,[a] Lionel Salmon,[a] Philippe Demont[d] and Azzedine Bousseksou*[a]

Received 23rd January 2012, Accepted 7th March 2012
DOI: 10.1039/c2cc30528c

We studied the spin state dependence of the electrical conductivity of the spin crossover compound [Fe(Htrz)$_2$(trz)](BF$_4$) (Htrz = 1*H*-1,2,4-triazole) by means of dc electrical measurements. The low spin state is characterized by higher conductance and lower thermal activation energy of the conductivity, when compared to the high spin state.

Spin-crossover (SCO) complexes of 3d^4–3d^7 transition metal ions are paradigmatic examples of molecular materials showing bistability in magnetic, optical and electrical properties.[1] The high spin (HS) ↔ low spin (LS) transition can be triggered by various external stimuli, such as temperature, light illumination, pressure or magnetic field, providing scope for applications in sensor, display, information storage and photonic devices.

A number of recent inspiring papers focused on the transport properties of SCO materials at the single molecule or nanoparticle level, in relation with interesting perspectives for the application of these compounds in molecular electronics and in spintronics.[2–6] Unfortunately, the characterization of such molecular devices by other means than $I = f(V)$ measurements is extremely difficult, leading—in *each* of the above cases—to a rather high uncertainty whether the observed current intensity changes occur due to a spin state conversion or other phenomena. This difficulty is considerably increased by the fact that it is not trivial to extrapolate to the single object level the different physical properties observed on a macroscopic ensemble. The same is true obviously for the charge transport mechanism. Theoretical calculations of the transport properties will certainly provide a useful help, but they are still in early stages of development. For these reasons, the different discussions in the literature regarding the spin state dependence of the electrical conductivity of SCO materials remain—at best—very speculative.

To progress in the understanding of this open question it is perhaps preferable to investigate for a first time a macroscopic sample[7,8] providing higher current levels and—even more importantly—easier sample characterization by a variety of standard techniques. To this aim we carried out variable-temperature dc conductivity measurements on the powder samples **C1**–**C3** of the [Fe(Htrz)$_2$(trz)](BF$_4$) complex (Fig. 1) synthesized by three different methods. (Sample synthesis and characterization methods are detailed in the ESI.†) The morphology of the three powder samples was characterized by scanning and transmission electron microscopies (see ESI†). Sample **C2** is composed of needle-like crystallites of typically 3–5 μm in length and *ca.* 200–300 nm in diameter. On the other hand, samples **C1** and **C3** are composed of nanometric particles of roughly spherical and rod-like shapes, respectively. It is important to note that while **C1** formed always vast aggregates, it was possible to obtain only weakly aggregated deposits from the ethanol suspensions of **C3**. The sample compositions were verified using IR and Raman spectroscopies as well as powder X-ray diffraction (pXRD) and were found to be very similar (see ESI†). Variable temperature Raman and ^{57}Fe Mössbauer spectra were used to confirm the spin state change in each sample and revealed a virtually complete and reversible transition (see ESI†). The thermal spin transition curves were determined by optical reflectivity (Fig. 1). **C1** and **C2** exhibit a thermal hysteresis of *ca.* 25 K, while the transition temperatures differ by about 10 K. Interestingly, the nanoparticle sample **C3** exhibits the largest hysteresis of ∼42 K. These differences might arise for several reasons: due to the different morphology, the presence of different structural defects and/or different degrees of hydration. The dc conductivity measurements have

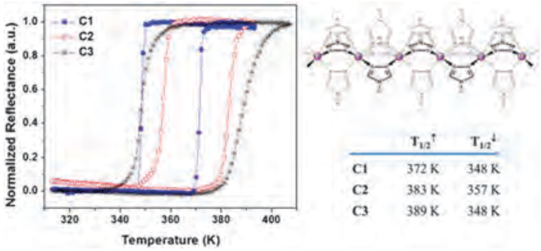

	$T_{1/2}^{\uparrow}$	$T_{1/2}^{\downarrow}$
C1	372 K	348 K
C2	383 K	357 K
C3	389 K	348 K

Fig. 1 General schematic structure of the Fe^{II}–triazole chain and the thermal spin transition curves of samples **C1–C3** together with the corresponding transition temperatures in the heating and cooling modes.

---

[a] *Laboratoire de Chimie de Coordination, CNRS UPR-8241 and Université de Toulouse, UPS, INP, F-31077 Toulouse, France. E-mail: azzedine.bousseksou@lcc-toulouse.fr*
[b] *Faculty of Electrical Engineering and Computer Science, Stefan cel Mare University, 13 Str. Universitatii, Suceava 720229, Romania*
[c] *Department of Chemistry, National Taras Shevchenko University, 62 Vladimirska str, 01601 Kiev, Ukraine*
[d] *LPP-CIRIMAT, CNRS & Université de Toulouse III, 118 Route de Narbonne, 31062 Toulouse, France*

† Electronic supplementary information (ESI) available: Experimental details, Raman and IR spectra, Mossbauer spectra, SEM, TEM and AFM images, XRD patterns, Arrhenius plots. See DOI: 10.1039/c2cc30528c

been performed in two-probe geometry. The powders of **C1** and **C2** (~0.2 mm thickness) were contained in a Teflon sample holder between two stainless steel electrodes. The particles of **C3** have been dispersed in ethanol and deposited on the electrode by spin-coating. Atomic force microscopy (AFM) measurements on the deposited sample revealed a discontinuous layer of about 100–150 nm in thickness with only a few aggregates. Hence, the data obtained for this sample correspond closely to the conduction through single particles and small aggregates of 2–3 nanoparticles.

By recording the electrical conductivity in the heating and cooling modes, each sample (**C1–C3**) reveals, reproductively, a large thermal hysteresis of σ_{dc} (Fig. 2), which can be assigned obviously to the spin transition properties.

When the temperature increases, the conductivity of **C1** is strongly thermally activated and drops abruptly at around 372 K by ~2 orders of magnitude. At 365 K, *i.e.* within the hysteresis region, the conductivity is 1.2×10^{-11} Sm^{-1} in the LS state and 1.7×10^{-13} Sm^{-1} in the HS state. The conductivity of sample **C2** is significantly higher when compared to **C1**, but the (relative) conductivity change associated with the spin transition is much smaller ($\sigma_{dc}^{LS} = 2.2 \times 10^{-9}$ Sm^{-1}, $\sigma_{dc}^{HS} = 1.3 \times 10^{-9}$ Sm^{-1}). The spin state dependence of the conductivity was detected even through very thin samples, in which the electrodes are separated by typically 1–2 particles only (sample **C3**). This observation suggests that the conductivity hysteresis is essentially the property of the particles and not dominated by grain boundary contribution. The thermal activation energy of the electrical conductivity in both the LS and HS states was determined for samples **C1** and **C2** using the Arrhenius equation:

$$\sigma_{dc} = \sigma_0 e^{-\frac{E_a}{k_B T}} \qquad (1)$$

where σ_0 is the pre-exponential factor, E_a is the activation energy and k_B is the Boltzmann constant. E_a can be calculated from the slope of the plot ln[$\sigma(T)$] *vs.* $1/T$ (see ESI†). In Table 1 one can see that the activation energy values are smaller in the LS state when compared to the HS state for both compounds. On the other hand, the pre-exponential factor presents very different behaviors. Sample **C1** is characterized by approximately the same value of the pre-exponential factors in the two spin states, while in sample **C2** σ_0 is very high and increases by three orders of magnitude when going from the LS to the HS state. It is worth stressing here that such huge difference between **C1** and **C2** occurs even though the composition, structure and spin crossover properties of the two samples were found to be very similar.

Table 1 Pre-exponential factors and activation energies of the conductivity in the LS and HS states

	σ_0^{LS}/Sm^{-1}	σ_0^{HS}/Sm^{-1}	E_a^{LS}/eV	E_a^{HS}/eV
C1	$6.0(2) \times 10^{-7}$	$9.2(2) \times 10^{-7}$	0.34(2)	0.52(4)
C2	$6.1(1) \times 10^{-4}$	$5.0(4) \times 10^{-1}$	0.52(1)	0.87(1)

The small value of the electrical conductivity suggests that the charge transport takes place by polaron hopping. One possible origin of the dc conductivity change is a hopping distance and/or hopping frequency modulation due to the change of the relevant phonon frequencies. Indeed, in the HS state the metal–ligand bond lengths are higher, leading to an overall shift of the vibrational density of states to lower frequencies.[2] Hence, the phonon contribution is more important in the LS state than in the HS state, which could explain the higher value of the electrical conductivity in the LS state. In the case of hopping transport, the Einstein diffusion relation is often used to connect the dc conductivity with the hopping frequency:

$$\sigma_{dc} = \frac{n_c(ea)^2}{6k_B T}\vartheta_p = \frac{n_c(ea)^2}{6k_B T}\vartheta_{0p}\exp\left[\frac{-E_p}{k_B T}\right] \qquad (2)$$

where n_c is the carrier density, e is the electronic charge, a is the hopping distance, ν_p is the hopping frequency, ν_{0p} is the phonon frequency and E_p is the activation energy of the hopping process (typically $E_p = E_a$).[9] One can see that the value of the pre-exponential factor is obtained by the competition of two terms: the hopping distance (which is larger in the HS state) and hopping frequency (which is higher in the LS state). The variation of the hopping activation energy with the electronic structure change is even more complex.[10] Depending thus on the microscopic details of the charge carrier hopping one may expect rather different behaviors when comparing different SCO compounds and even in the same compound with different defects and morphology. Here it is worth noting also that the energy gap between the HS and LS states is typically less than 40–50 meV, *i.e.* much smaller than the activation energy of the electrical conductivity (~500 meV). Therefore, the fact that in the HS state the electrons are unpaired should not play any important role in the thermal activation process of the electrical conductivity; all the more it is not sure whether the electrons of the iron ions would participate in the charge transport. One should also note that the SCO can also induce in certain cases a structural phase transition and may be difficult to separate the contributions of the two phenomena to the conductance change. According to the combined pXRD and Raman study

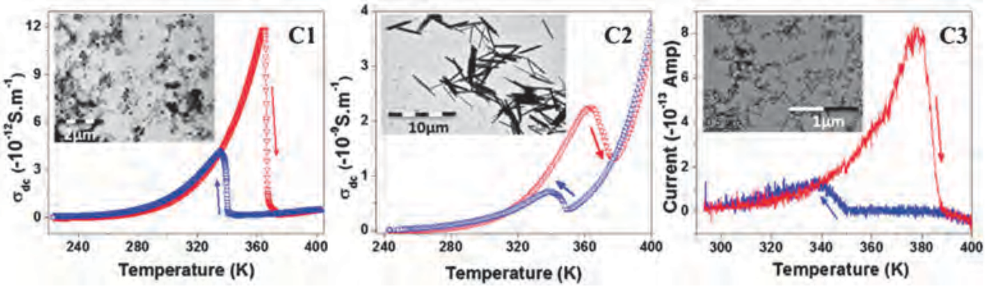

Fig. 2 Temperature dependence of the dc electrical conductivity of compounds **C1** (left) and **C2** (middle) in the heating (red) and cooling (blue) modes. For **C3** (right) we show the $I = f(T)$ curve because the conductivity could not be determined accurately (see ESI† for details). The insets show typical TEM images of the samples (see also ESI†).

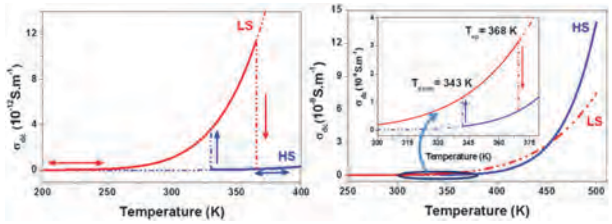

Fig. 3 Calculated temperature dependence of the electrical conductivity in the LS and HS states for samples **C1** (left) and **C2** (right).

of Urakawa *et al.*,[11] however, the spin transition does not trigger such structural transition in the compound [Fe(Htrz)$_2$(trz)](BF$_4$). Since we used the same synthesis method and we obtained very similar Raman and pXRD spectra (see ESI†) we can plausibly discard this hypothesis in our study.

Using the obtained values for the pre-exponential factors and thermal activation energies for samples **C1** and **C2** we plotted, using the Arrhenius law, the temperature dependence of the conductivity calculated in the two spin states (Fig. 3). One can observe that the presence (or the absence) of the spin state dependence of the electrical conductivity is conditioned by three key parameters: the values of switching temperatures *vs.* the activation energy of the electrical conductivity, the difference between the activation energies in the LS and HS states and the difference between the pre-exponential factors in the two spin states. Of course, one should not omit that other parameters such as the abruptness of the transition will influence also the observation of the spin state change through conductivity measurements.

The results in Fig. 3 allow us to explain why the thermal spin state dependence of the conductivity has not been seen in other samples of the same family, reported in ref. 12. Indeed, this is clearly related to the fact that the activation barriers are too high compared to the thermal energy available in the temperature range around the switching temperatures and the electrical conductivity cannot be activated. Thus, the electrical conductivity will be close to zero in both the LS and HS states. A very interesting role in the spin state dependence of the conductivity is played by the pre-exponential factors. In sample **C2** the pre-exponential factors are much higher in the HS state than in the LS state, which suggests that the conductivity is much faster thermally activated in the HS state than in the LS state. This leads to a crossing of the conductivity of the two states: at low temperatures the LS state has higher conductance due to the lower activation energy, while at high temperatures the inverse behavior occurs due to the differences in σ_0. Depending thus on the temperature at which the spin transition occurs one can observe either a more conductive LS state or a more conductive HS state. For example, the application of an external pressure should allow us to shift the spin transition above this crossing point and thus to observe experimentally the inversion of the conductivity between the two spin states.

In summary, we have observed a thermal hysteresis loop in the dc electrical conductivity of the compound [Fe(Htrz)$_2$(trz)](BF$_4$), which is clearly associated with the molecular spin state switching phenomenon. We have found that the conductivity of this compound is much higher in the LS phase—due to the lower activation barrier in this state. Perhaps even more importantly, we have also shown that the modification of the synthesis conditions can drastically modify the charge transport behavior of the complex and can even inverse the sign of the conductivity change, albeit the spin crossover properties remain nearly unaltered. We can conclude thus that small changes in the defect structure or in the particle morphology (grain boundary effects) may lead to a dramatic change in the conductance behavior and even its mechanism can be modified; making unreliable theoretical predictions whether the HS or LS state is more conductive. Our results also highlight that the possibility to observe the spin state dependence of the conductivity in the intrinsically highly insulating SCO compounds depends above all on the interplay between the spin transition temperature and the activation parameters. Finally, we have shown, in an irrefutable way, that the thermal dependence of the electrical conductance is measurable for 100 nm SCO particles, which is promising for the elaboration of nanoelectronic and spintronic devices based on SCO nano-objects. Let us mention also that electrical measurements seem to be a very promising characterization tool in the study of the size effect in single SCO objects and it should be underlined that strong size and spin-state dependence of the transport behavior is expected when approaching the tunneling regime.

Financial support from the project ANR Crossnanomat is acknowledged. The work at Suceava was supported by the project PRiDE, Contract No. POSDRU/89/1.5/S/57083, a project cofounded from the European Social Fund through Sectorial Operational Program Human Resources.

Note added after first publication: this article replaces the version published on 08 March 2012, which contained errors in the references list.

Notes and references

1 A. Bousseksou, G. Molnar, L. Salmon and W. Nicolazzi, *Chem. Soc. Rev.*, 2011, **40**, 3313.

2 C. Etrillard, V. Faramarzi, J.-F. Dayen, J.-F. Létard and B. Doudin, *Chem. Commun.*, 2011, **47**, 9663.

3 M. S. Alam, M. Stocker, K. Gieb, P. Muller, M. Haryono, K. Student and A. Grohmann, *Angew. Chem., Int. Ed.*, 2010, **49**, 1159.

4 V. Meded, A. Bagrets, K. Fink, R. Chandrasekar, M. Ruben, F. Evers, A. Bernand-Mantel, J. S. Seldenthuis, A. Beukman and H. S. J. van der Zant, *Phys. Rev. B: Condens. Matter Mater. Phys.*, 2011, **83**, 245415.

5 F. Prins, M. Monrabal-Capilla, E. A. Osorio, E. Coronado and H. S. J. van der Zant, *Adv. Mater.*, 2011, **23**, 1545.

6 D. Aravena and E. Ruiz, *J. Am. Chem. Soc.*, 2011, **134**, 777.

7 L. Salmon, G. Molnar, S. Cobo, P. Oulie, M. Etienne, T. Mahfoud, P. Demont, A. Eguchi, H. Watanabe, K. Tanakae and A. Bousseksou, *New J. Chem.*, 2009, **33**, 1283.

8 T. Mahfoud, G. Molnar, S. Cobo, L. Salmon, C. Thibault, C. Vieu, P. Demont and A. Bousseksou, *Appl. Phys. Lett.*, 2011, **99**, 053307.

9 G. Molnar, S. Cobo, T. Mahfoud, E. J. M. Vertelman, P. J. van Koningsbruggen, P. Demont and A. Bousseksou, *J. Phys. Chem. C*, 2009, **113**, 2586.

10 D. R. Rosseinsky and J. S. Tonge, *J. Chem. Soc., Faraday Trans. 1*, 1982, **78**, 3595.

11 A. Urakawa, W. Van Beek, M. Monrabal-Capilla, J. Ramon Galan-Mascaros, L. Palin and M. Milanesio, *J. Phys. Chem. C*, 2011, **115**, 1323.

12 A. Bousseksou, G. Molnar, P. Demont and J. Menegotto, *J. Mater. Chem.*, 2003, **13**, 2069.